




Comparison of needle arthroscopy, traditional arthroscopy, and computed tomography for the evaluation of medial coronoid disease in the canine elbow

Rebecca A. Hersh-Boyle DVM¹ | Po-Yen Chou BVM, MS, DACVS-SA²  |
 Amy S. Kapatkin DVM, MAS, DACVS² |
 Mathieu Spriet DVM, MS, DACVR, DECVDI² |
 Barbro Filliquist DVM, DACVS-SA, DECVS²  | Tanya C. Garcia MS² |
 Denis J. Marcellin-Little DEDV, DACVS, DACVSMR² 

¹William R Prichard Veterinary Medical Teaching Hospital, School of Veterinary Medicine, University of California Davis, Davis, California

²Department of Surgical and Radiological Sciences, School of Veterinary Medicine, University of California Davis, Davis, California

Correspondence

Po-Yen Chou, Department of Surgical and Radiological Science, School of Veterinary Medicine, University of California Davis, One Shields Ave, Davis, CA 95616.
 Email: pchou@ucdavis.edu

Funding information

Center of Companion Animal Health, School of Veterinary Medicine, University of California, Davis, Grant/Award Number: 2016-51-R

[Correction added on 18 February 2021, after first online publication: acknowledgement updated.]

Abstract

Objective: To evaluate the diagnostic value of still images of needle arthroscopy (SNAR), still images of traditional arthroscopy (STAR), and computed tomography (CT) to diagnose medial coronoid process (MCP) pathology.

Study design: Prospective clinical trial.

Animals: Dogs (n = 17) presented for evaluation of elbow dysplasia.

Methods: For each case, two SNAR and STAR images of the MCP were reviewed independently and in random order by three board-certified surgeons. Computed tomographic images were reviewed by one board-certified radiologist. Reviewers were blinded to surgical and clinical findings. Surgical findings from real-time TAR with palpation were used as the gold standard. Receiver operating characteristic (ROC) curves and concordance statistics tests for the diagnostic accuracy of MCP fissure, MCP fragment, medial compartment condition, and cartilage score were calculated.

Results: Images of 27 elbows joints were reviewed. For MCP fissure detection, areas under the ROC curves for CT (0.84), STAR (0.73), and SNAR (0.57) did not differ. For the detection of MCP fragment, STAR had a larger area under the ROC curve (0.93) compared with SNAR (0.74, $P = .015$) and CT (0.54, $P < .001$). Still images of TAR and SNAR had comparable concordance for cartilage score (0.80 and 0.77, respectively) and medial compartment pathology (0.80 and 0.73, respectively).

Conclusion: Still images of NAR, STAR, and CT had similar diagnostic value to identify MCP fissures. Still images of TAR was superior to SNAR and CT to identify MCP fragments.

Clinical significance: The diagnostic accuracy of SNAR varied on the basis of the coronoid lesion being evaluated.

1 | INTRODUCTION

Elbow dysplasia is a collective term describing several inheritable diseases of which medial coronoid disease (MCD) is the most prevalent form.¹ Medial coronoid disease is characterized by lesions of the medial coronoid process (MCP), including chondromalacia, fragmentation, fissures, or abnormal shape.^{2,3} While different lesions may lead to different surgical or nonsurgical management and prognosis, orthopedic examination and radiographs alone cannot discern the type of pathologic lesion present.²

Cross-sectional imaging modalities such as computed tomography (CT) and MRI have improved the identification of lesions of MCD.⁴⁻⁶ Cross-sectional imaging has limitations, including high cost, limited availability, and limited value to characterize cartilage integrity.⁴ Surgical evaluation with traditional arthroscopy (TAR) has been considered to be the gold standard for identifying the magnitude and severity of MCD.³ Because of the cost of the procedure and the requirement for general anesthesia, the arthroscopic diagnosis and treatment commonly take place during a single anesthetic episode.

Needle arthroscopy (NAR) is used in human medicine as a diagnostic tool that has been described as an alternative to MRI for the characterization of disease severity.⁷ It has been used as an outpatient procedure with patients under local anesthesia to investigate joint problems in man and horses.⁷⁻¹² The use of NAR in dogs presented with MCD has not been previously investigated.

The objective of this study was to evaluate the diagnostic value of still images of NAR (SNAR), and compare it to still images of TAR (STAR) and CT. We hypothesized that SNAR, STAR, and CT would have equivalent accuracy for the diagnosis of MCP pathology.

2 | MATERIALS AND METHODS

2.1 | Case selection

Client-owned dogs weighing more than 20 kg referred to our institution with a presumptive diagnosis of MCD between May 2017 and November 2018 were candidates for inclusion. Dogs were excluded when local skin lesions were present over the medial aspect of the elbow, an ununited anconeal process was present, or > 2 mm of radioulnar incongruity was detected by CT.¹³ The study protocol was approved by the University of California Davis IACUC (protocol No. 19791). Signed informed consent was obtained from owners before enrollment.

2.2 | Sedation

Dogs were sedated for CT and NAR. The sedation protocol included 5 to 7.5 µg/kg of dexmedetomidine (Zoetis, Parsippany, New Jersey) given IV in combination with 0.05 to 0.1 mg/kg of hydromorphone (Baxter Healthcare Corporation, Deerfield, Illinois) or in combination 0.1 to 0.2 mg/kg of butorphanol (Zoetis).

2.3 | Computed tomography

Computed tomography of both elbows extending from the mid-humerus to the distal antebrachium was performed with a 16-slice CT scanner (GE LightSpeed; GE, Boston, Massachusetts). Dogs were positioned in dorsal recumbency with elbow joints flexed at 90°. Images were acquired with field of view ranging in size from 9.6 to 22 cm, slice thickness of 1.2 mm, peak kilovoltage of 120 kVp, and intensity of 180 mA, and were reconstructed into 0.6-mm-thick sections by using a bone algorithm.

2.4 | Preparation for NAR and TAR

One board-certified surgeon (P.Y.C.) performed all NAR and TAR procedures. The medial elbow regions were clipped, scrubbed, and prepared for an aseptic procedure. Needle arthroscopy was performed prior to general anesthesia. Anesthesia was induced, and TAR was performed. Standardized video recording and still images were acquired within each elbow joint for both techniques.

2.5 | Needle arthroscopy

For NAR, dogs were positioned in dorsal recumbency with the affected limb held in abduction, exposing the medial aspect of the elbow. The distal humerus was placed on a sandbag to serve as a fulcrum, and pressure was applied to the antebrachium to distract the medial elbow joint space. A fenestrated adhesive transparent drape (Steri-Drape; 3 M Health Care, St Paul, Minnesota) was placed over the elbow joint.

The NAR portal was established by inserting an 18-gauge (1 mm) hypodermic needle into the elbow joint, approximately 1 cm distal and 5 mm caudal to the medial epicondyle. Five to 10 mL of sterile lactated Ringer's solution (Baxter Healthcare Corporation) was injected to distend the joint space. A No. 11 scalpel blade was used to make a 2-mm skin incision around the needle. The NAR unit, a 0°, 14-gauge (1.6 mm) system featuring an outer

needle sheath and an inner scope/camera design (mi-eye 2; Trice Medical, Malvern, Pennsylvania), was inserted into the joint after removal of the needle. The outer sheath of the NAR unit was retracted to allow visualization. An egress portal was established by inserting an 18-gauge needle adjacent to the anconeal process. Lactated Ringer's solution with an IV administration set (10 drops/mL) in a pressure infusion bag (Infusable; Vital Signs, Totowa, New Jersey) was used for joint distention and irrigation through the ingress portal of the NAR unit. The pressure infusion bag was pressurized to allow for adequate visualization. Still images of the anconeal process, the trochlear notch, the MCP, the radial head, and the medial aspect of the humeral condyle were acquired with the NAR unit. The NAR unit and the egress needle were removed, and the skin incision was sealed with cyanoacrylate glue (Surgical Adhesive; VetOne, Boise, Idaho).

2.6 | Traditional arthroscopy

For TAR, dogs were positioned in dorsal recumbency with the affected limb held in abduction, exposing the medial aspect of the elbow. The distal humerus was placed on a sandbag to serve as a fulcrum, with the limb placed into a custom-made elbow distractor to maintain positioning. A standard four-corner drape (Utility Drapes; Haylard Health, Alpharetta, Georgia) and a fenestrated adhesive transparent drape (3 M Health Care) were placed over the elbow joint. The TAR portals and egress were established by using a previously reported technique.¹⁴ Lactated Ringer's solution was delivered through the arthroscopic cannula with a peristaltic pump (DualWave arthroscopy pump; Arthrex Vet Systems, Naples, Florida) at a delivery pressure of 45 mm Hg. Still images were acquired for TAR evaluation with a 1.9-mm 30° arthroscope (Synergy HD arthroscopic system; Arthrex Vet Systems). Anatomic locations evaluated included the anconeus process, trochlear notch, MCP, radial head, and medial aspect of the humeral condyle.

2.7 | Surgical findings

After image acquisition, an intraoperative arthroscopic assessment was performed with the 1.9-mm 30° arthroscope inserted by using a blunt trocar. The MCP was palpated for the presence of step or mobile fragment to reach the diagnosis of a medial coronoid fragment or fissure, with the aid of a 1.5-mm arthroscopic probe (Arthrex Vet Systems). Surgical findings were documented and used as gold standard for the analyses. The

ulnar articular surface along the scope portal was evaluated for iatrogenic cartilage damage. Iatrogenic cartilage damage was classified as NAR related, TAR related, or undetermined according to its shape, location, and direction. When elbow joint pathology was present, it was treated. The arthroscope was removed, and the skin incisions were closed with simple interrupted skin sutures.

2.8 | Evaluation of diagnostic modalities

Four matched MCP images (two from NAR and two from TAR) from each elbow were selected for evaluation by three board-certified veterinary surgeons (A.S.K., B.F., D.J.M.) with practice limited to small animal orthopedics. Still images of NAR and STAR images were reviewed in random order (www.randomizer.org). The images were anonymized, and the reviewers were blinded to the dogs' signalment, CT findings, surgical findings, arthroscopic treatment, and the findings of other reviewers. The reviewers graded four aspects of the medial coronoid: the presence of a fissure, the presence of a fragment, the health of the cartilage of the MCP, and the general condition of the medial compartment. A fissure of the MCP was defined as an abnormality of the MCP without clear separation or displacement of the MCP.¹⁵ An MCP fragment was defined as a free fragment that was detached and potentially displaced. Fissures and fragments were each graded as definitely absent, possibly present, probably present, likely present, or definitely present (Figure 1). The general condition of the medial compartment was graded as normal, possibly abnormal, probably abnormal, likely abnormal, or abnormal (Figure 2). Cartilage damage was graded according to the modified Outerbridge scoring system (MOS), ranging from normal to grade V lesions.¹⁵ Two reviewers (A.S.K., B.F.) repeated the evaluation of the SNAR and STAR images at least 4 weeks after the initial evaluation.

2.9 | Computed tomographic evaluation

A board-certified specialist of the American College of Veterinary Radiology (M.S.) reviewed the CT images of each elbow. The reviewer was blinded to SNAR and STAR image findings, surgical findings, and the arthroscopic treatments performed. The reviewer graded the CT evaluation of the MCP in two categories, presence of an MCP fissure and presence of an MCP fragment. A fissure was defined as a radiolucent line within the MCP without clear separation or displacement of the MCP. A fragment was defined as a free fragment that was detached and displaced. Fissures and fragments of the MCP were graded

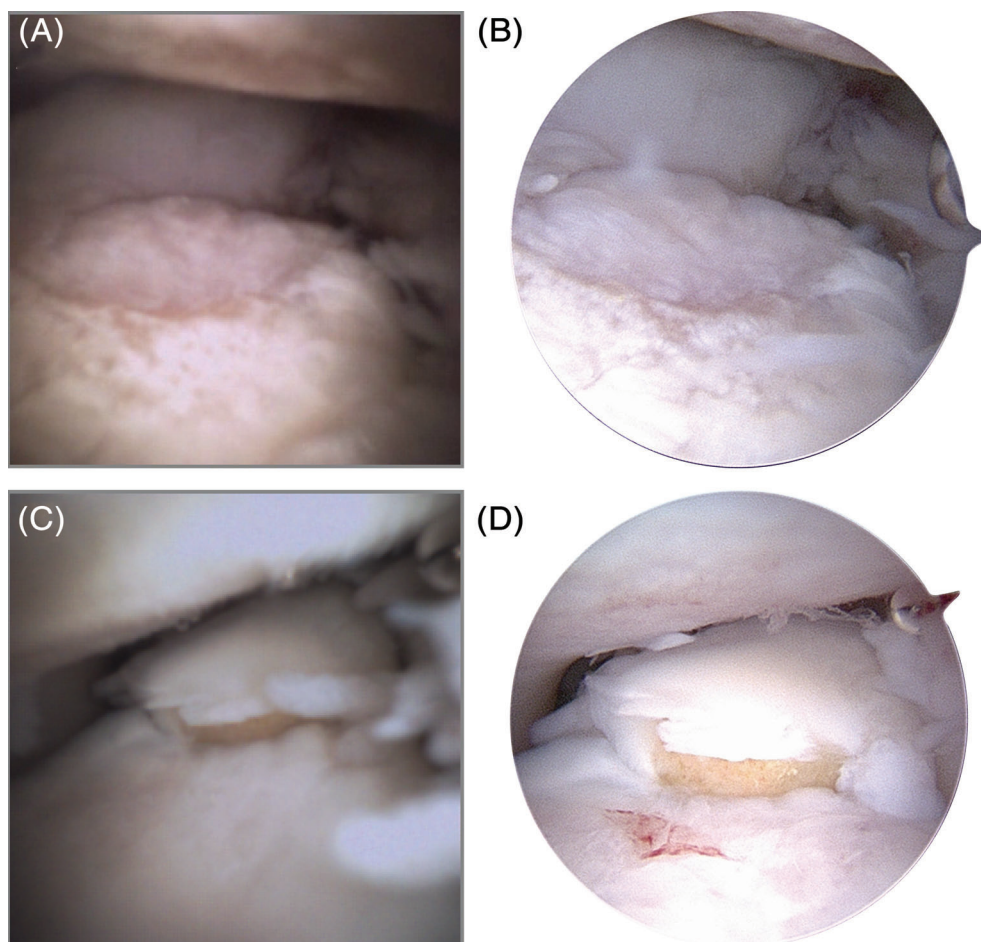


FIGURE 1 A,B, Images of the medial coronoid process (MCP) of a 5-year-old Labrador retriever acquired during needle arthroscopy (NAR; A) and traditional arthroscopy (TAR; B) of the elbow joint. A surgical diagnosis of fissure of the MCP was reached. The NAR and the TAR images were read as probable presence of fissure by three examiners. C,D, Images of the MCP of a 1-year-old golden retriever acquired during NAR (C) and TAR (D) of the elbow joint. A surgical diagnosis of fragment of the MCP was reached. The NAR and the TAR images were read as definitely present of fragment by three examiners. The NAR images were acquired as squares with resolution of 250×250 pixels, for a total of 62 500 pixels per image. Traditional arthroscopy images were circles with a resolution of approximately 1000 pixels along the diameter of the picture, for a total of approximately 800 000 pixels per image

as definitely absent, possibly present, probably present, likely present, or definitely present.³

2.10 | Statistical analysis

A power analysis was performed to detect a difference in the mean severity score of joint disease in the elbow of 1 out of 5 at a power of 0.8 and an α of .05. The power analysis yielded a sample size of 31 elbow joints. Statistical analysis was performed in SAS v 9.4 (SAS Institute, Cary, North Carolina). Grades between the first and second evaluations of two reviewers were compared to determine intraobserver reliability. Grades from the three reviewers were compared to determine interobserver agreement, calculated by using intraclass correlation coefficients (ICC). An ICC value <0.5

indicated poor agreement, a value ≥ 0.5 and < 0.75 indicated moderate agreement, a value ≥ 0.75 and < 0.9 indicated good agreement, and a value ≥ 0.9 indicated excellent agreement.¹⁶ The median value of the allocated grades by using CT, SNAR, and STAR image findings were compared to intraoperative arthroscopic findings by using of receiver operating characteristic (ROC) curve analysis. The sensitivity of STAR, SNAR and CT to detect an MCP fissure and MCP fragment at specificities of 80%, 90%, and 95% were calculated in R (R Foundation for Statistical Computing, Vienna, Austria. <http://www.R-project.org/>).¹⁷⁻¹⁹ Concordance statistics (c-statistic; area under the ROC curves) were compared statistically. C-statistic values ranged from 0.5 to 1. Values of 0.5 indicated random predictions, and values of 1 indicated perfect predictions.²⁰ Significance was set at $P < .05$.

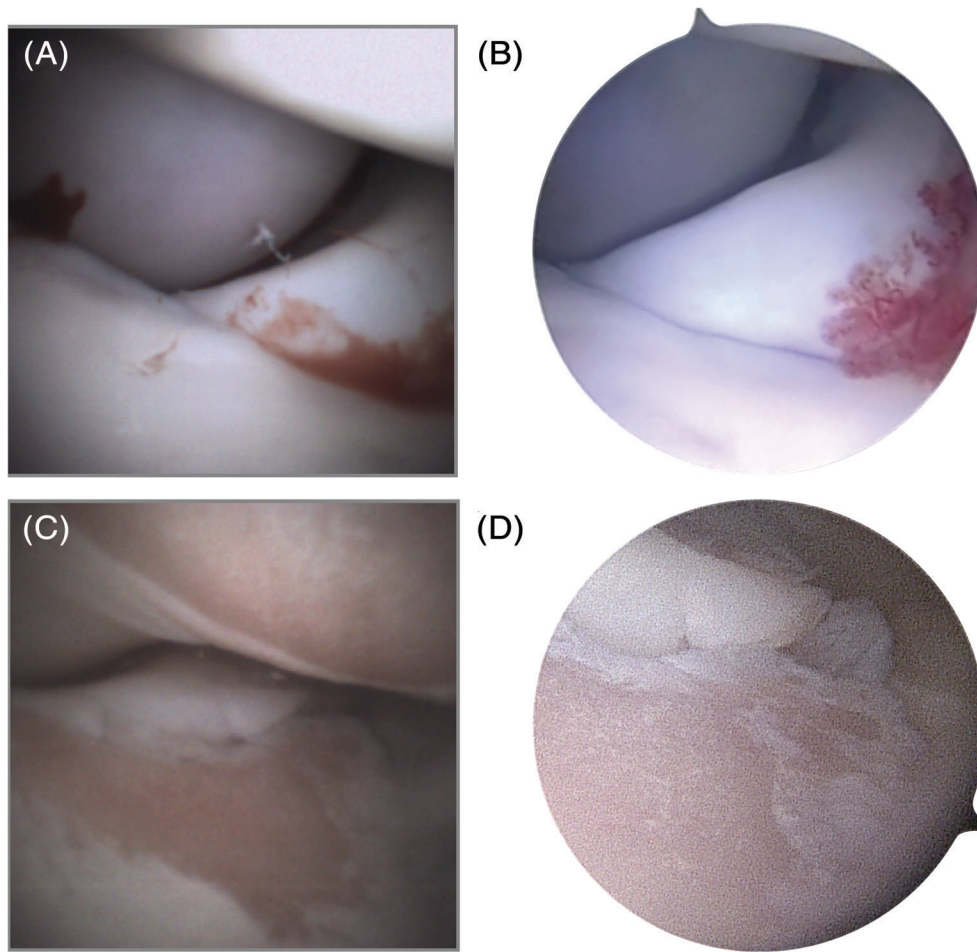


FIGURE 2 A,B, Images of the medial compartment of the elbow joint of a 7-month-old Labrador retriever acquired during needle arthroscopy (NAR; A) and traditional arthroscopy (TAR; B). The surgical diagnosis was humeral osteochondrosis dissecans with mild medial coronoid process chondromalacia and medial compartment disease. The NAR and the TAR images were interpreted as probably abnormal and likely abnormal, respectively by three examiners. C,D, Images of the articular surface of the medial coronoid process of a 5.7-year-old German shepherd acquired during NAR (C) and TAR (D) of the elbow joint. The surgical diagnosis was a grade V modified Outerbridge score lesion. The interpretation of the NAR and traditional images by three examiners was a grade III-IV modified Outerbridge score lesion. The NAR images were acquired as squares with resolution of 250×250 pixels, for a total of 62 500 pixels per image. Traditional arthroscopy images were circles with a resolution of approximately 1000 pixels along the diameter of the picture, for a total of approximately 800 000 pixels per image

3 | RESULTS

Thirty-one elbow joints from 17 dogs met the inclusion criteria, and 27 joints were included in the final statistical analyses. Four joints were excluded, three because successful introduction of the needle arthroscope could not be achieved despite multiple attempts (up to three attempts), and one because appropriate STAR images were not available. Median age of dogs was 1.8 years (range, 0.6-9), and median body weight was 29.9 kg (range, 20-42 kg). Partial-thickness cartilage damage was identified in six elbow joints. In four joints, the damage was NAR related, and, in two joints, the damage was caused by the needle used for joint distention for NAR or

TAR. The surgical diagnoses included MCP fragments in 16 elbow joints, MCP fissures in five elbow joints, and no MCP fragment or fissure in six elbow joints. The operative MOS of the MCP was 0 in two dogs, 1 in five dogs, 2 in nine dogs, 3 in four dogs, 4 in five dogs, and 5 in two dogs, with a median MOS of 2 (range, 0-5). Medial compartment evaluation was graded as abnormal in all elbow joints.

3.1 | Fissure identification

The area under the ROC curve for fissure detection was 0.84 for CT (95% CI, 0.74-0.94), 0.73 for STAR (95% CI,

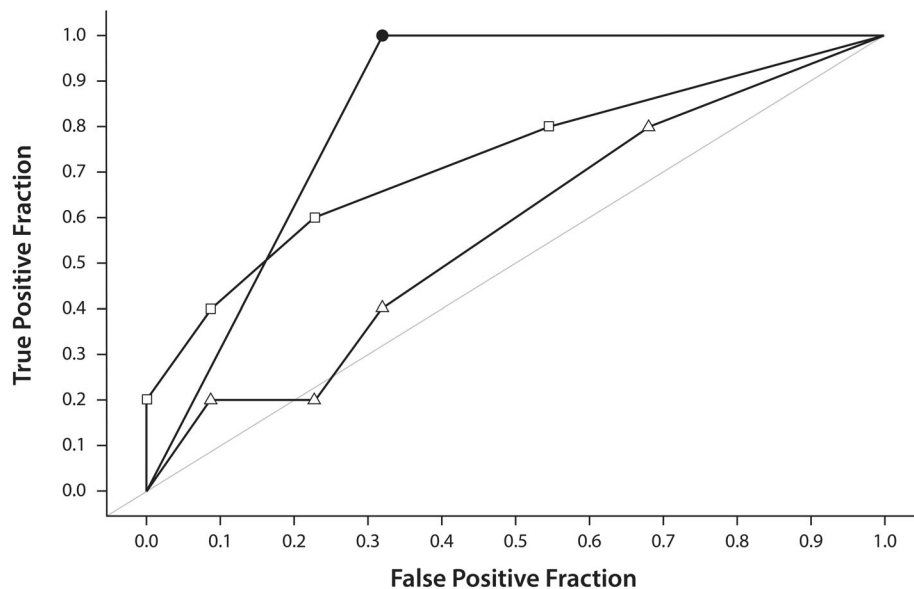


FIGURE 3 Receiver operating characteristic (ROC) curves for detection of fissure of the medial coronoid process by use of still images of traditional arthroscopy (STAR; open squares), still images of needle arthroscopy (SNAR; open triangles), and computed tomography (CT; solid circle) in 27 elbow joints of 17 clinically affected dogs. The y axis represents the sensitivity, and the x axis represents one minus the specificity of each test. The oblique gray line illustrates a random test with an area under the curve of 0.5. The curves were drawn on the basis of the median values of three independent readers of SNAR and STAR and the value of one CT reader, using surgical findings as a gold standard. The areas under the ROC curves were 0.84 for CT, 0.73 for STAR, and 0.57 for SNAR

TABLE 1 Areas under the receiver operating characteristic curve for the identification of a fissure and fragment of the medial coronoid process and c-statistic analysis for cartilage and medial compartment condition, using surgical findings as gold standard

Modality	Fissure	Fragment	Cartilage evaluation	Medial compartment
STAR	0.73	0.93 ^a	0.80	0.80
SNAR	0.57	0.74 ^b	0.77	0.73
CT	0.84	0.55 ^b	N/A	N/A

Abbreviations: c-statistic, concordance statistic; CT, computed tomography; N/A, not applicable; SNAR, still images of needle arthroscopy; STAR, still images of traditional arthroscopy.

^aThe area under curve was significantly larger than that of SNAR ($P = 0.015$) and CT ($P < 0.001$).

^bNo significant differences between SNAR and CT.

TABLE 2 Intraobserver and interobserver reliability of TAR and NAR for the evaluation of 27 canine elbow joints with elbow dysplasia

Modality	Intraobserver agreement				Interobserver agreement			
	MCP fissure	MCP fragment	MOS cartilage	Medial compartment	MCP fissure	MCP fragment	MOS cartilage	Medial compartment
STAR	0.916	0.916	0.857	0.857	0.687	0.837	0.763	0.658
SNAR	0.677	0.877	0.892	0.646	0.628	0.788	0.856	0.720

Abbreviations: MCP, medial coronoid process; MOS, modified Outerbridge score; SNAR, still images of needle arthroscopy; STAR, still images of traditional arthroscopy.

0.44-1), and 0.57 for SNAR (95% CI, 0.28-0.85; Figure 3, Table 1). These areas under the ROC curve did not differ. For the detection of an MCP fissure, the sensitivity of STAR was 55.6% at a specificity of 80%, 42.4% at a specificity of 90%, and 32.1% at a specificity of 95%. The sensitivity of

SNAR was 26.4% at a specificity of 80%, 13.2% at a specificity of 90%, and 6.4% at a specificity of 95%. The sensitivity of CT was 59.0% at a specificity of 80%, 30.7% at a specificity of 90%, and 15.5% at a specificity of 95%. Intraobserver agreement for detection of a fissure was excellent for STAR

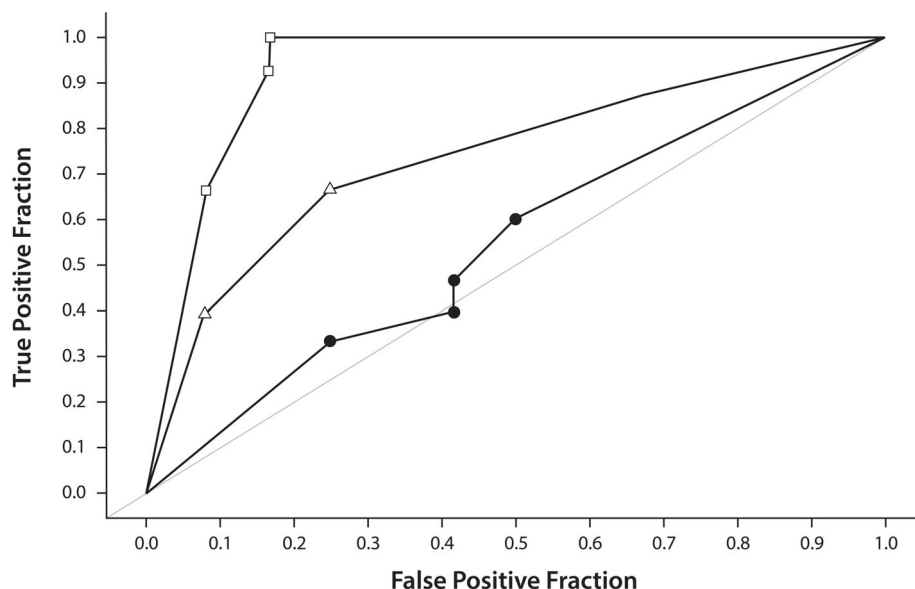


FIGURE 4 Receiver operating characteristic (ROC) curves for detection of fragment of the medial coronoid process by use of still images of traditional arthroscopy (STAR; open squares), still images of needle arthroscopy (SNAR; open triangles), and computed tomography (CT; solid circle) in 27 elbow joints of 17 clinically affected dogs. The y axis represents the sensitivity, and the x axis represents one minus the specificity of each test. The oblique gray line illustrates a random test with an area under the curve of 0.5. The curves were drawn on the basis of the median values of three independent readers of SNAR and STAR and the value of one CT reader, using surgical findings as a gold standard. The areas under the ROC curves were 0.93 for still images of traditional arthroscopy, 0.74 for still images of needle arthroscopy, and 0.55 for computed tomography

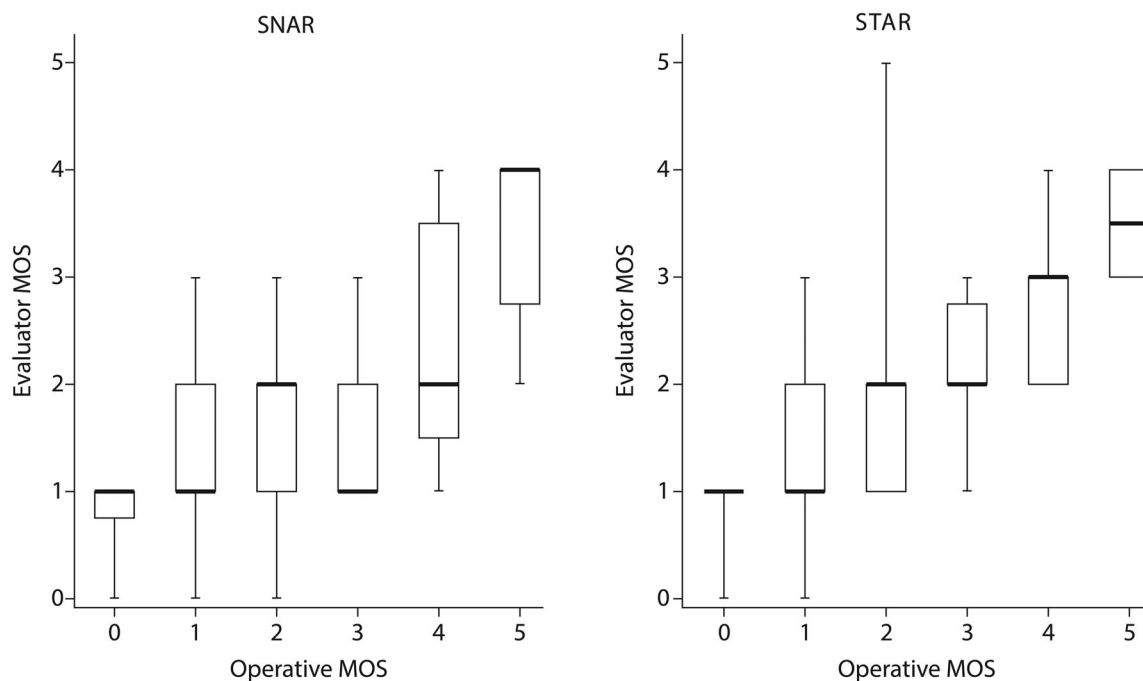


FIGURE 5 Box-and-whisker plots of modified Outerbridge score (MOS) assessed with still images of needle arthroscopy (SNAR) and still images of traditional arthroscopy (STAR) among the three evaluators. The x axis represents the operative arthroscopy MOS grading, and the y axis represents the MOS grading by the evaluators. For each box, the thick line illustrates the median value, and the upper and lower boundaries illustrate the second and third quartiles, respectively. Whiskers illustrate the minimal and maximal values

and moderate for SNAR. Interobserver agreement was moderate for STAR and for SNAR (Table 2).

3.2 | Fragment identification

The area under the ROC curve for fragment detection was 0.93 for STAR (95% CI, 0.81-1), 0.74 for SNAR (95% CI, 0.44-0.93), and 0.55 for CT (95% CI, 0.33-0.76; Figure 4, Table 1). The area under the ROC curve for STAR was larger than that for SNAR ($P = .015$) and CT ($P < .001$). Still images of NAR and CT did not differ. For the detection of an MCP fragment, the sensitivity of STAR was 96.6% at a specificity of 80%, 75.6% at a specificity of 90%, and 40.4% at a specificity of 95%. The sensitivity of SNAR was 57.8% at a specificity of 80%, 44.6% at a specificity of 90%, and 34.0% at a specificity of 95%. The sensitivity of CT was 21.6% at a specificity of 80%, 9.8% at a specificity of 90%, and 4.3% at a specificity of 95%. Intraobserver agreement for the detection of a fragment was excellent for STAR and good for SNAR. Interobserver agreement for the detection of a fragment was good for STAR and for SNAR (Table 2).

3.3 | Cartilage evaluation

Still images of TAR and SNAR had moderate agreement with the surgical evaluation of cartilage pathology (Figure 5). Intraobserver agreement for cartilage pathology was good for STAR and excellent for SNAR. Interobserver agreement for cartilage pathology was good for STAR and for SNAR.

3.4 | Evaluation of the medial compartment of the elbow

Still images of TAR and SNAR had moderate agreement with the surgical evaluation of medial compartment pathology. Intraobserver agreement for medial compartment evaluation was good for STAR and moderate for SNAR. Interobserver agreement for medial compartment evaluation was moderate for STAR and for SNAR.

4 | DISCUSSION

We rejected the hypothesis that still images of NAR and TAR and CT images would provide evidence to diagnose MCD with equivalent accuracy. The diagnostic accuracy of SNAR varied according to the lesion being evaluated. Still

images of NAR was less accurate than STAR for the detection of a fragmented MCP. However, the diagnostic values of SNAR and STAR for the detection of an MCP fissure did not differ statistically. Also, SNAR and STAR had similar value when evaluating cartilage pathology and the general condition of the medial compartment of the elbow.

Needle arthroscopy is performed as an outpatient procedure in human medicine without the requirement of using general anesthesia.¹⁰ In the current study, SNAR was intentionally performed under sedation to determine the diagnostic value of the test when it was used as an outpatient procedure. Only dogs weighing >20 kg were included in the study because most dogs presented to our institution with elbow dysplasia are medium or large breed dogs. Subjectively, the learning curve involved in the use of NAR initially resulted in prolonged time required for system set up, animal transportation, and positioning. This may have led to suboptimal sedation in the dogs treated early in the study. Dogs that were less sedated may have had more muscle tone, negatively impacting animal positioning and full joint distention. These were likely factors leading to difficulties in accessing the joints in three cases early in the study. With additional experience, setup and positioning times were reduced, and, subjectively, the ease of joint access was increased.

The MOS grading scheme was adapted from a previous study in dogs and allowed grading of cartilage health without arthroscopic palpation.¹⁵ Because of the study design, palpation was not performed during NAR procedures because probing was not deemed possible with dogs under sedation, and manipulation of lesions may have altered the final operative diagnostic result. Palpation would likely have improved the diagnostic value in the fragment identification and differentiation between MOS 0 and MOS1 lesions during SNAR evaluation.

Cartilage damage occurred in six of 27 elbow joints. Four lesions were caused by NAR insertion. Needle arthroscopy evaluated in this study uses a retractable needle design, which included a 14-gauge (1.6 mm) outer sheath and a camera within the sheath. By comparison, the insertion for the TAR uses a blunt trocar, which may lead to a safer insertion. In addition, sedation in the NAR group may also have led to increased muscle tone and, thus, likely resulted in decreased joint space opening and increased risk of cartilage damage during sheath insertion.

The images exported from the NAR and the TAR systems used in the present study had a notable difference in resolution and a visible notch that is characteristic of the angled arthroscope; therefore, it was not possible for the reviewers to be truly blinded to the modalities used for image acquisition. Still images of NAR and STAR were evaluated together in random order, and all

identifying animal information was removed. Being able to differentiate between the two modalities may have had a more significant impact on the result if the experiment were designed by using a binomial result (sensitivity and specificity), which would have failed to account for the diagnostic value of each diagnostic modality. In the present study, a graded system was used and evaluated by using ROC analysis and c-statistic to fully characterize the diagnostic value of each diagnostic modality. Receiver operating curve analysis determines the diagnostic value of a test across the range of sensitivity and specificity regardless of tester personality. When a tester performs a test with an aggressive approach, sensitivity increases but specificity decreases. Conversely, when a tester tentatively performs a test, sensitivity decreases but specificity increases. The area under an ROC curve (c-statistic) is not influenced by tester personality during the evaluation of a test.^{20,21}

The identification of a fissure, as defined in this study, required the identification of a narrow, nondisplaced, discontinuity of the MCP. Computed tomography had the greatest numerical diagnostic value to detect fissures, although that value did not differ statistically from TAR and NAR. Computed tomography is likely to be the best modality for fissure detection because it evaluates subchondral bone integrity and may allow for the identification of MCP fissures even with normal overlying cartilage. Diagnosis of MCP fissures with normal overlying cartilage during surgical evaluation would require palpation with an arthroscopy probe, which was not achievable during the evaluation of STAR and SNAR in the present study. These findings are in agreement with another study in 141 joints with elbow dysplasia in which MCD was identified by CT in all joints, including fissures without visible cartilage pathology during arthroscopy.²² Alternatively, the presence of a cartilage fissure with intact subchondral bone could also lead to a discrepancy between CT and arthroscopic assessment of the MCP.²³

The identification of an MCP fragment relies on the ability to detect a detached or displaced portion of the MCP. Traditional arthroscopy identified MCP fragments better than NAR and CT. Traditional arthroscopy images were obtained with dogs positioned under general anesthesia, which may have allowed better positioning of the joint (ie, pronation) and may have influenced fragment displacement. Differences in image quality may also have contributed to these findings. The NAR unit collected images at a resolution of 250×250 pixels when an integrated camera/arthroscope design was used, whereas the TAR unit collected images with a resolution of 1280×720 pixels when a rod-lens optical design was used, an approximately 10-fold increase in resolution.¹⁰ In addition, the needle

arthroscope is a 0° scope with a 120° field of view and 5 to 35 mm of focal depth. Hoshino et al²⁴ showed in a two-dimensional human knee model that a 0° arthroscope had greater image distortion compared to a 30° arthroscope at a shallow distance and straight viewing angle. To minimize distortion when a 0° arthroscope is used, the arthroscope should be perpendicular to the object being viewed.²⁵ When the MCP is evaluated from a portal distal to the medial humeral condyle with NAR, the needle scope cannot be perpendicular to the area of the elbow evaluated and may lead to distortion. Image distortion of the integrated camera/arthroscope design used in the present study has not been evaluated and should be a future area of study. In the present study, use of a cranial scope portal may have allowed for direct viewing of the MCP with a better visualization of lesions with less distortion. Evaluation of a different portal position was not performed because it would require a different study design that was beyond the objectives of the current study. The needle arthroscope is designed with an integrated ingress attached to a syringe or a fluid line. In the current study, NAR was performed with a gravity pump, and TAR was performed with an automated pump. Needle arthroscopy has a smaller ingress sheath diameter and may have led to the requirement for higher pressure to maintain adequate fluid flow required for visualization. Automated pumps have been shown to enhance image quality during human arthroscopic procedures by reducing the amount of turbidity by 50% compared to gravity pumps.²⁶ Researchers in a cadaveric study performed in canine stifle joints also concluded that arthroscopic peristaltic pumps allowed improved viewing of intra-articular structures with less extra-articular fluid accumulation than when fluid was delivered by a pressure bag.²⁷

Computed tomography had the lowest diagnostic accuracy for MCP fragments in this study, whereas it had the highest accuracy for fissure detection. This discrepancy seems counterintuitive, but a likely explanation is that CT relies purely on osseous changes, whereas STAR and SNAR assess primarily the cartilaginous surface. In the present study, the evaluator was asked to determine whether a displaced fragment was present, and multiple factors may have contributed to the lack of confidence in the diagnosis of definite fragmentation. Most likely, CT may not have been able to accurately differentiate minimally displaced MCP fragments from MCP fissures, leading to a higher accuracy for the detection of fissures and a lower accuracy for the detection of fragments. In a previous study, CT had 93% sensitivity and 100% specificity to diagnose MCP pathology, but half of the minimally displaced MCP fragments

were misidentified as fissures.²² Also, some MCP fragments may have been cartilaginous.²³ Without the involvement of subchondral bone, these fragments would not have been detectable by CT. The CT resolution possibly did not allow accurate detection of small MCP fragments, despite the use of thin slices. With severe sclerosis and local remodeling, visualization of displaced fragments may be more challenging. Finally, fragments potentially were more readily differentiated during arthroscopic evaluation because of the magnifying effect of the arthroscopy. In another study, CT failed to identify lesions in 29% of elbow joints with MCP fragments (displaced and nondisplaced).⁴

Clinically, the management of a displaced fragment could differ from the management of a minor fissure.²⁸ For example, the biceps ulnar release procedure has been recommended when only mild radial incisure fissure is present and the dog has only mild clinical signs.²⁸ Identification of a displaced fragment has been reported to be associated with cartilage erosion of the MCP and medial humeral condyle⁴ and may alter the surgeon's decision to perform a proximal ulnar osteotomy.²⁸ Currently, the evidence is not clear whether the absence or presence of medial coronoid fragment or medial coronoid fissure affect the prognosis for patients presented with different degrees of cartilage disease. Computed tomography and SNAR had similar diagnostic values in identifying a displaced fragment in our study. The use NAR under sedation may allow for better surgical planning and client communication.

The moderate agreement of STAR and SNAR with surgical findings when cartilage lesions and overall conditions of the medial compartment of the elbow were characterized may have resulted from the use of still images to evaluate TAR and NAR relative to the use of video for the surgical assessment. Still images were chosen to minimize the variability between TAR and NAR and allow for anonymization and randomization. Still images do not provide the same detail that real-time video assessment provides²⁹ because the three-dimensional evaluation of the MCP is eliminated; this could account for a loss of agreement between SNAR, STAR, and surgical findings.

The ability to characterize the degree of cartilage damage prior to definite operative arthroscopy treatment may help in treatment planning and provide a basis for prognosis and follow-up recommendations in dogs with elbow dysplasia.²⁸ In two studies,^{30,31} arthroscopic surgical treatment and nonsurgical treatment resulted in similar long-term treatment outcomes, evaluated prospectively by gait analysis³⁰ and retrospectively by responses to an owner questionnaire.³¹ Both studies were limited by the use of International Elbow Working Group score for the characterization of the elbow pathology, which had been reported to be a sensitive but less specific indicator of cartilage

pathology.¹⁵ To better categorize elbow joint pathology and correlate with treatment outcomes, a precise presurgical diagnostic tool would be ideal. Computed tomography had only moderate correlation between osteophytosis and the location and degree of arthroscopic pathology, and absence of CT-confirmed pathology does not preclude cartilage disease.^{4,32} Magnetic resonance imaging may be a great tool and is commonly used in human medicine to identify cartilage lesion; however, the reported correlation between MRI and arthroscopic Outerbridge score is only moderate, with a ρ score of 0.404.³² Needle arthroscopy with video assessment may have the highest diagnostic value in identifying cartilage lesions among the presently available preoperative diagnostic tools that can be performed under sedation and can potentially help further investigation of elbow dysplasia treatments as well as guide clinical decision making for the treatment of elbow dysplasia.

The lower intraobserver reliability for SNAR compared to STAR for the identification of a fissure and for the evaluation of the general condition of the medial compartment of the elbow is likely related to the decreased image quality of SNAR relative to STAR. Both of these categories rely on a detailed evaluation of the joint cartilage to make an accurate assessment. As previously discussed, the image quality of SNAR was lower than that of STAR because of the use of a gravity pump, lower resolution, and the 0° angle of the NAR. The moderate interobserver reliability of STAR and SNAR may have resulted from the use of a five-point grading system rather than a continuous scale (eg, visual analog scale) to detect subtle changes. In a study in which arthroscopy of the human knee was evaluated, a continuous scale had higher interobserver reliability compared with a five-point scale.³³ Clinical experience and demeanor of the readers also influence interobserver reliability. Cartilage evaluation had high interobserver and intraobserver reliability for STAR and for SNAR. That reliability may have been increased by the absence of normal elbow joints in the study.

This study had limitations. The nature of a clinical trial precluded the inclusion of normal joints. Normal elbows or dogs with no forelimb lameness have no indication for diagnostic tests of this nature. Therefore, all elbows included in this study had elbow pathology. Inclusion of normal elbows in the study may have yielded a different result. The images for STAR evaluation were obtained immediately before surgical evaluation with dogs under the same joint position, which could have led to an analytical advantage for STAR compared with SNAR. A single radiologist evaluated CT. Having a single rater could have increased the skewness of the CT ROC curve.²¹ Finally, the relatively small sample and the evaluation of still images may have led to large confidence intervals, relatively low power, and possible type II error

during statistical analyses. A larger sample would have enhanced the ability to detect small diagnostic differences between methods.

In conclusion, the results of this study provide evidence that NAR can identify and characterize elbow medial compartment pathology as well as the severity of cartilage lesions before surgical or nonsurgical treatment of elbow dysplasia. Computed tomography maybe a preferred diagnostic modality for the identification of additional fissures but may not be the optimal modality for differentiating nondisplaced and displaced fragments. Needle arthroscopy and CT can be used as outpatient diagnostic tools that can successfully be performed under sedation.

ACKNOWLEDGMENTS

The authors would like to thank Chrisoula Toupadakis Skouritakis, PhD for assistance with illustrations.

AUTHOR CONTRIBUTIONS

Hersh-Boyle RA, DVM: Obtained research grant for the study. Assisted in data collection. Created blinded image sets for evaluation. Drafted, revised, and approved the submitted manuscript; Chou PY, BVM, MS, DACVS-SA: Conception of the study, study design. Obtained client consent for study. Collected all arthroscopic, CT, and surgical finding data. Interpretation of the result. Drafted, revised, and approved the submitted manuscript; Kapatkin AS, DVM, MAS, DACVS: Contributed to the concept of the study and study design, reviewed all SNAR and STAR images. Revised, and approved the submitted manuscript; Spriet M, DVM, MS, DACVR, DECVDI: Contributed to the conception of the study and study design, reviewed all CT images. Revised, and approved the submitted manuscript; Filliquist B, DVM, DACVS-SA, DECVS: Contributed to the conception of the study and study design reviewed all SNAR and STAR images. Revised, and approved the submitted manuscript; Garcia TC, MS: Performed statistical analysis. Revised, and approved the submitted manuscript; Marcellin-Little DJ, DEDV, DACVS, DACVSMR: Contributed to the conception of the study and study design, reviewed all SNAR and STAR images. Performed statistical analysis. Drafted, revised, and approved the submitted manuscript.

CONFLICT OF INTEREST

The authors report no financial or personal conflicts of interest related to this report.

ORCID

Po-Yen Chou  <https://orcid.org/0000-0002-0344-5465>
 Barbro Filliquist  <https://orcid.org/0000-0001-6116-6520>
 Denis J. Marcellin-Little  <https://orcid.org/0000-0001-6596-5928>

REFERENCES

1. Lavrijsen ICM, Heuven HCM, Voorhout G, et al. Phenotypic and genetic evaluation of elbow dysplasia in Dutch Labrador Retrievers, Golden Retrievers, and Bernese mountain dogs. *Vet J*. 2012;193:486-492.
2. Fitzpatrick N, Smith TJ, Evens RB, Yeadon R. Radiographic and arthroscopic findings in the elbow joints of 263 dogs with medial coronoid disease. *Vet Surg*. 2009;38:213-223.
3. Lau SF, Theyse LFH, Voorhout G, Hazewinkel HAW. Radiographic, computed tomographic, and arthroscopic findings in Labrador Retrievers with medial coronoid disease: imaging and arthroscopic findings with medial coronoid disease. *Vet Surg*. 2015;44:511-520.
4. Moores AP, Benigni L, Lamb CR. Computed tomography versus arthroscopy for detection of canine elbow dysplasia lesions. *Vet Surg*. 2008;37:390-398.
5. Cook CR, Cook JL. Diagnostic imaging of canine elbow dysplasia: a review. *Vet Surg*. 2009;38:144-153.
6. Snaps FR, Park RD, Saunders JH, Balligand MH, Dondelinger RF. Magnetic resonance arthrography of the cubital joint in dogs affected with fragmented medial coronoid processes. *Am J Vet Res*. 1999;60:190-193.
7. Quinn R, Lang SD, Gilmer BB. Diagnostic needle arthroscopy and partial medial meniscectomy using small bore needle arthroscopy. *Arthrosc Tech*. 2020;9:e645-e650.
8. Deirmengian CA, Dines JS, Vernace JV, Schwartz MS, Creighton RA, Gladstone JN. Use of a small-bore needle arthroscope to diagnose intra-articular knee pathology: comparison with magnetic resonance imaging. *Am J Orthop*. 2018; 47. <https://doi.org/10.12788/ajo.2018.0007>.
9. Daggett MC, Stepanovich B, Geraghty B, Meyers A, Whetstone J, Saithna A. Office-based needle arthroscopy: a standardized diagnostic approach to the shoulder. *Arthrosc Tech*. 2020;9:e521-e525.
10. McMillan S, Saini S, Alyea E, Ford E. Office-based needle arthroscopy: a standardized diagnostic approach to the knee. *Arthrosc Tech*. 2017;6:e1119-e1124.
11. Kadic DTN, Miagkoff L, Bonilla AG. Needle arthroscopy of the radiocarpal and middle carpal joints in standing sedated horses. *Vet Surg*. 2020;49:445-454.
12. Frisbie DD, Barrett MF, McIlwraith CW, Ullmer J. Diagnostic stifle joint arthroscopy using a needle arthroscope in standing horses: diagnostic stifle joint arthroscopy. *Vet Surg*. 2013;43:12-18.
13. Kramer A, Holsworth IG, Wisner ER, Kass PH, Schulz KS. Computed tomographic evaluation of canine radioulnar incongruence in vivo. *Vet Surg*. 2006;35:24-29.
14. Beale BS, Hulse DA, Schulz KS, Whitney WO. *Small Animal Arthroscopy*. Philadelphia, PA: Elsevier; 2003.
15. Farrell M, Heller J, Solano M, Fitzpatrick N, Sparrow T, Kowaleski M. Does radiographic arthrosis correlate with cartilage pathology in Labrador Retrievers affected by medial coronoid process disease? *Vet Surg*. 2014;43:155-165.
16. Koo TK, Li MY. A guideline of selecting and reporting intraclass correlation coefficients for reliability research. *J Chiropr Med*. 2016;15:155-163.
17. Robin X, Turck N, Hainard A, et al. pROC: an open-source package for R and S+ to analyze and compare ROC curves. *BMC Bioinformatics*. 2011;12:77. <https://doi.org/10.1186/1471-2105-12-77>.

18. Carter JV, Pan J, Rai SN, Galandiuk S. ROC-ing along: evaluation and interpretation of receiver operating characteristic curves. *Surgery*. 2016;159:1638-1645.
19. Turner DA. An intuitive approach to receiver operating characteristic curve analysis. *J Nucl Med*. 1978;19:213-220.
20. Steyerberg EW, Harrell FE, Borsboom GJJM, Eijkemans MJC, Vergouwe Y, Habbema JDF. Internal validation of predictive models. *J Clin Epidemiol*. 2001;54:774-781.
21. Chanoit G, Singhani NN, Marcellin-Little DJ, Osborne JA. Comparison of five radiographic views for assessment of the medial aspect of the humeral condyle in dogs with osteochondritis dissecans. *Am J Vet Res*. 2010;71:780-783.
22. Villamonte-Chevalier A, van Bree H, Broeckx B, et al. Assessment of medial coronoid disease in 180 canine lame elbow joints: a sensitivity and specificity comparison of radiographic, computed tomographic and arthroscopic findings. *BMC Vet Res*. 2015;11:243.
23. Ryssen BV, van Bree H. Arthroscopic findings in 100 dogs with elbow lameness. *Vet Rec*. 1997;140:360.
24. Hoshino Y, Rothrauff BB, Hensler D, Fu FH, Musahl V. Arthroscopic image distortion—part I: the effect of lens and viewing angles in a 2-dimensional in vitro model. *Knee Surg Sports Traumatol Arthrosc*. 2014;24:2065-2071.
25. Hoshino Y, Rothrauff BB, Hensler D, Fu FH, Musahl V. Arthroscopic image distortion—part II: the effect of lens angle and portal location in a 3D knee model. *Knee Surg Sports Traumatol Arthrosc*. 2014;24:2072-2078.
26. Tuijthof GJM, van den Boomen H, van Heerwaarden RJ, van Dijk CN. Comparison of two arthroscopic pump systems based on image quality. *Knee Surg Sports Traumatol Arthrosc*. 2008;16:590-594.
27. Warnock JJ, Nemanic S, O'Donnell MD, Wiest JE. Comparison of 2 fluid ingress/egress systems for canine stifle arthroscopy using computed tomography. *Vet Surg*. 2014;43:944-951.
28. Fitzpatrick N, Yeadon R. Working algorithm for treatment decision making for developmental disease of the medial compartment of the elbow in dogs. *Vet Surg*. 2009;38:285-300.
29. Burton NJ, Owen MR, Kirk LS, Toscano MJ, Colborne GR. Conservative versus arthroscopic management for medial coronoid process disease in dogs: a prospective gait evaluation. *Vet Surg*. 2011;40:972-980.
30. Dempsey L, Maddox T, Comerford E, Pettitt R, Tomlinson A. A comparison of owner-assessed long-term outcome of arthroscopic intervention versus conservative management of dogs with medial coronoid process disease. *Vet Comp Orthop Traumatol*. 2019;32:1-9.
31. Haudiquet PR, Marcellin-Little DJ, Stebbins ME. Use of the distomedial-proximolateral oblique radiographic view of the elbow joint for examination of the medial coronoid process in dogs. *Am J Vet Res*. 2002;63:1000-1005.
32. Wavreille V, Fitzpatrick N, Drost WT, Russell D, Allen MJ. Correlation between histopathologic, arthroscopic, and magnetic resonance imaging findings in dogs with medial coronoid disease. *Vet Surg*. 2015;44:501-510.
33. Ayrat X, Gueguen A, Ike RW, et al. Interobserver reliability of the arthroscopic quantification of chondropathy of the knee. *Osteoarthritis Cartilage*. 1998;6:160-166.

How to cite this article: Hersh-Boyle RA, Chou P-Y, Kapatkin AS, et al. Comparison of needle arthroscopy, traditional arthroscopy, and computed tomography for the evaluation of medial coronoid disease in the canine elbow. *Veterinary Surgery*. 2021;1–12. <https://doi.org/10.1111/vsu.13581>